

Preparation and characterization of a stable nano-CoAl₂O₄ ink for glass decoration by ink-jet printing

PENG Xiaojin^{1, 2}, ZHANG Qi^{3, 4*}, CHENG Jinshu^{1, 2}, YUAN Jian^{1, 2}, WU Ya^{1, 2}, JIE
Junnan^{1, 2}

¹State Key Laboratory of Silicate Materials for Architectures, Wuhan University of
Technology, Wuhan, 430070, Hubei, China

²Glass and Technology Research Institute of Shahe, Shahe, 054100, Hebei, China

³State Key Laboratory of Advanced Technology for Materials Synthesis and
Processing, Wuhan University of Technology, Wuhan 430070, Hubei, China

⁴School of Aerospace, Transportation and Manufacturing, Cranfield University,
Cranfield, Bedfordshire, MK430AL, UK

Abstract: A stable inorganic glass ink was prepared by mechanically grinding a mixture of a blue pigment (CoAl₂O₄) and low-melting-point glass powders in a specific organic solvent, which possesses a lower annealing temperature compared with ceramic ink. The CoAl₂O₄ was synthesized by solid-state reaction and the best sintering temperature should be at 1300 °C or above according to the observation of XRD. CoAl₂O₄ shows blue color both in a powder form and coating. The average particle size of pigments and glass powders mixture decreases with the increase of glass powders and milling time. SEM cross-sectional

* Corresponding author. Tel.: 44 (0) 1234 750111; Fax: 44 (0) 1234 751346
E-mail address: Q.Zhang@cranfield.ac.uk

1 images of annealed coating samples illustrate that the pigments are well
2
3 dispersed in the ink layer and the glass adhesive binds well on the surface
4
5 of plate glass materials, enhancing the mechanical strength of the ink
6
7 layer. All the obtained results collectively revealed that the prepared
8
9 nano-CoAl₂O₄ ink can be applied in glass decoration.
10
11
12
13
14
15
16
17
18
19
20
21

22 **Keywords:** Nano-CoAl₂O₄ ink; Preparation; Characterization; Ink-jet
23
24 printing; Glass decoration
25
26
27
28
29
30
31
32
33
34
35
36
37
38
39
40
41
42
43
44
45
46
47
48
49
50
51
52
53
54
55
56
57
58
59
60
61
62
63
64
65

1 Introduction

Ink-jet printing is a non-contact digital printing technology, which can deposit a variety of materials, as droplets, on pre-determined points of a substrate under the control of a computer program. [1~5] One important aspect of ink-jet printing applications is to develop corresponding inks, in which a solute or pigment is dispersed in an organic solvent, with appropriate physical and chemical properties, such as viscosity, surface tension and drop volume of ink and so on. [6~8] Additionally, the use of nano-sized pigments in ink-jet printing system avoids some problems occurring, for example, nozzle clogging and dispersion instability, and thus ensures the quality of printing products. [9~13]

Recently, with an increasing demand of home and public places decorations, colorful patterns on glass tiles with high resolution have attracted the attention of most consumers in the market. The glass decorating materials are often deposited on glasses by means of spin-coating, dip-coating, drop-casting and screen printing previously. However, ink-jet printing as a non-contact deposition method can exhibit obvious advantages over other methods, for instance, a low cost, high definition, efficient use of materials, compatibility with different substrates and its precise when quickly transferring the inks on the surface of substrates. [14] Unfortunately, the reports in the literatures on

1 glass inks are relatively rare in comparison with ceramic inks. Thus
2
3 developing a proper nano-sized inorganic glass ink is essential to ensure
4
5 the operation of ink-jet printing process.
6
7

8
9 Most of the early researching works focused on the preparation of
10
11 ceramic inks and various preparation methods, for example, Guo et al.
12
13 [15] prepared the four colors (CMYK) ceramic inks for ink-jet printing
14
15 by sol-gel method; Domingo et al. [16] prepared a ceramic pigment based
16
17 on Cr and Sb doped TiO_2 by a microemulsion mediated solvothermal
18
19 method; both Merikhi et al. [17] and Dondi et al. [18] prepared
20
21 nano-sized CoAl_2O_4 particles by the polyol method; Kim et al. [19]
22
23 prepared well-dispersed nanoparticles of CoAl_2O_4 for ink-jet printing by a
24
25 hydrothermal process with ultrasonic irradiation; Kuscer et al. [20]
26
27 prepared an aqueous titania suspension for ink-jet printing by mechanical
28
29 grinding method, and so on. Although all these inks are successfully
30
31 applied in printing on ceramics, they fail to perform well on glasses
32
33 because the surface structures of ceramic and glass are totally different,
34
35 the former porous and the latter dense. The different surface structures
36
37 can result in diverse solvent volatilization of ink droplet and discrepant
38
39 coloring effect. What's more, taking the annealing temperature of printed
40
41 substrates into consideration, ceramic substrates allow the annealing at a
42
43 very high temperature which is easy to cause softening and bending
44
45 deformation of glass substrates.
46
47
48
49
50
51
52
53
54
55
56
57
58
59
60
61
62
63
64
65

This paper focuses on the preparation of a nano-sized blue glass ink, in which cobalt aluminum oxide (CoAl_2O_4) is served as a blue pigment, with the aim of annealing ink-jet printed blue materials on glass substrates at relatively low temperatures. CoAl_2O_4 is an oxide that contains two metallic elements in a spinel structure, where Co^{2+} ions are located in tetrahedral positions and Al^{3+} ions are sited in octahedral positions. [21~22] Powders of CoAl_2O_4 synthesized by solid-state reaction have a unique optical characteristic and excellent resistance to light and harsh environment. The addition of low-melting-point glass powders to the ink could reduce the annealing temperature, enhance the adhesion between pigment and glass substrate, and avoid the softening and bending deformation of glass substrate when annealed at high temperature.

2 Materials and Methods

2.1 Materials

Aluminum oxide (Al_2O_3), Cobalt (III) oxide (Co_2O_3) and Zinc oxide (ZnO) were provided by Sinopharm Chemical Reagent Co., Ltd, Shanghai, China. 1, 2-propyleneglycol diacetate, diethylene glycol monobutyl ether, polyacrylate, Zinc isoocatanoate isopropanol, ethyl alcohol and polysiloxane were purchased from Jianglai Biological Co., Ltd, Shanghai, China. The float glasses were used as substrates for coating.

1 All other chemicals used in this work were laboratory grade as received
2
3 from Sinopharm Company, China.
4
5

6 **2.2 Preparation of the blue glass inks and coated samples**

7

8
9 The mixtures of 16.6 g Cobalt oxide (Co_2O_3 , 0.1 mol), 20.4 g
10 Aluminum oxide (Al_2O_3 , 0.2 mol) and 1.62 g Zinc oxide (ZnO , 0.02 mol)
11 used for promoting blue coloration were added into 15mL ethyl alcohol
12 and mixed homogeneously into a slurry by milling.
13
14
15
16
17
18
19

20 Subsequently, the slurry was grinded manually for 30 minutes in air
21 until the ethyl alcohol evaporated completely. Following such steps, the
22 obtained mixture was calcined in an alumina crucible at different reaction
23 temperatures (900 °C, 1100 °C, 1200 °C and 1300 °C) for 4 hours in an
24 electrical furnace. The fired product underwent several cycles of grinding
25 and firing in order to achieve a good yield of the required crystalline
26 phase and acceptable homogeneity. The primary pigment (CoAl_2O_4) was
27 obtained when the temperature cooled down to the room temperature.
28
29
30
31
32
33
34
35
36
37
38
39
40
41

42 Additionally, low-melting-point glass, $\text{ZnO-B}_2\text{O}_3\text{-SiO}_2$ system, was
43 used as the glass adhesive to enhance the binding of primary pigments
44 and the surface of plate glass after annealed. Raw materials (ZnO , B_2O_3
45 and SiO_2 , and so on) of low-melting-point glass were mixed by milling
46 and fused in an alumina crucible at 1280 °C for 2 hours to form a high
47 temperature melt. After that, the melt was underwent water quenching
48 and grinded fully. The main chemical compositions of the four different
49
50
51
52
53
54
55
56
57
58
59
60
61
62
63
64
65

low-melting-point glasses (Glass Adhesives (GA1~4)) are given in Table 1, with various mass contents of TiO_2 and ZrO_2 . The addition of TiO_2 and ZrO_2 can enhance the chemical resistance of ink layer [23, 24], but too much TiO_2 and ZrO_2 would lead to crystallization of the glass adhesive, which will interfere the color of pigment [25~27].

Correspondingly, the primary pigments and low-melting-point glass powders were mixed and milled fully using a wet ball-milling method at room temperature to form the secondary pigments, which were filtered through a 50 μm sieve to remove larger particles and agglomerates. The resultant secondary pigments were dispersed in a special organic solvent with a vigorously stirring to prepare the homogeneous blue glass ink. Table 2 shows the main chemical compositions of the prepared blue glass ink.

Consequently, the glass substrates, which were cleaned with isopropanol as well as de-ionized water and dried under N_2 flow, were coated with the blue ink via drop-casting and then annealed in an electrical furnace at 580 $^\circ\text{C}$ for 10 minutes. Fig.1 shows the flowchart of the whole process of preparing the blue glass ink and glass surface coating.

2.3 Characterization of ink and coating

The $\text{CIE-L}^*\text{a}^*\text{b}^*$ values were measured by spectrophotometer CM-2600d, in which L^* is the lightness axis [black (0), white (100)], a^* is

the green (—) to red (+) axis, and b^* is the blue (—) to yellow (+) axis. The pH value, surface tension and viscosity of the prepared blue glass ink were measured by Mettler Toledo multi parameter test gauge, Rotary viscosimeter NDJ-5S and Surface tension meter DSAHT17-1, respectively. The crystal structures of primary and secondary pigments were examined by an X-ray diffraction (XRD, D/MAX-UItimaIV, Rigaku). The $\text{CuK}\alpha$ radiation ($\lambda = 0.15405 \text{ nm}$) was used at 40 kV and 40 mA. The diffraction patterns were recorded with $2\theta = 10 - 70^\circ$. The particle size distribution was measured by Mastersizer 2000 (Malvern Instruments) as well as SEM. The thermal expansion coefficients of the low-melting-point glasses were measured by thermal expansion analysis. The cross-sectional morphologies of the coated substrates were observed by SEM.

3 Results and discussion

3.1 Primary pigment – CoAl_2O_4

3.1.1 Effect of solid state reaction temperature on crystallization behavior by XRD analysis

Fig.2 shows the XRD patterns of the calcined pigments at different solid-state reaction temperatures. At 900 °C (Fig.1a), both CoAl_2O_4 and Co_3O_4 phases were identified according to their respective JCPD cards (No: 44-0160 and 38-0814) [28]. Increasing the reaction temperature to

1 1100 °C (Fig.1b), CoAl_2O_4 phase became dominant with the existence of
2
3 small amount of Al_2O_3 phase, which was almost invisible when the
4
5 reaction temperature was further increased to 1200 and 1300 °C (Fig.
6
7 1c&d). The phase analysis manifests that, below 1200 °C, the raw
8
9 materials of Al_2O_3 and Co_2O_3 with a molar ratio of 2:1 failed to form pure
10
11 CoAl_2O_4 but, confirmed by XRD, a solid solution of CoAl_2O_4 and Al_2O_3 .
12
13 Moreover, the intensity of the CoAl_2O_4 diffraction peaks was enhanced
14
15 and the diffraction peaks were sharpened with the increase of reaction
16
17 temperature from 1100 °C to 1300 °C, which were associated with an
18
19 increase in crystallinity.
20
21
22
23
24
25
26

27 28 29 **3.1.2 Chromatic analysis of the primary pigment against different** 30 31 **reaction temperatures** 32 33

34
35 Table 3 and Fig.3 show the colorimetric $L^*a^*b^*$ values and optical
36
37 pictures of the produced blue primary pigments and a coated sample. L^*
38
39 is the lightness axis [black (0), white (100)], a^* the green (—) to red (+)
40
41 axis, and b^* the blue (—) to yellow (+) axis. In fact, the yield of blue
42
43 color is mainly governed by parameter b^* : the more negative b^* value
44
45 corresponding to the bluer one. According to Fig.3 (a) ~ (d) and Table 1,
46
47 it's easily observed that more intense blue color pigments were achieved
48
49 when the sintering temperature was 1300 °C, which are indicated by the
50
51 extremely high blue component ($b^* = -24.51$) and a relatively low green
52
53
54
55
56
57
58
59
60
61
62
63
64
65

component ($a^* = -1.59$). [9] The color change by varying the reaction temperature was well evidenced by the evolution of colorimetric parameters. The color of primary pigment achieved at 900 °C (Fig. 3(a)) was near black while the color of primary pigment at 1100 °C (Fig. 3(b)) was about navy blue. When the reaction temperature increased from 1200 °C (Fig. 3(c)) to 1300 °C (Fig. 3(d)), the CoAl_2O_4 pigment presented a blue color with more lightness. The color changes of primary pigments at different temperatures can attribute to the existence of defects in spinel structure. These defects lead to the interchange between Al^{3+} and Co^{2+} in tetrahedral and octahedral sites which can change the ligand field around the chromophore and hence change the observed color. [29~31] In other word, if the preparation of CoAl_2O_4 by solid-state reaction method can be executed successfully, the sintering temperature would be about 1300 °C. Fig.3 (e) was the coating of primary pigment (d) on a glass substrate, which was annealed at 580 °C for 10 minutes. The color of the coating (e) is consistent with that of primary pigment (d), indicating that no color change of primary pigment occurred during the process of annealing.

3.2 Secondary pigments - CoAl_2O_4 mixed with glass adhesive

3.2.1 XRD analysis of low-melting-point glasses and secondary pigment

Fig. 4 (A) shows the XRD patterns of low-melting-point glass powders, and Fig.4 (B) shows XRD patterns of the primary pigment (d)

(see Table 3) and the secondary pigment (88%). The XRD pattern of primary pigment (d) indicates that CoAl_2O_4 is the main crystalline phase, with some unknown impurities, possibly being Co_2O_3 or/and Al_2O_3 . Low-melting-point glasses 1[#] ~ 4[#] are four different glass adhesives, and all the XRD spectra of them (Fig.4 (A)) show that no obvious diffraction peaks can be found indicating that they are amorphous and these glass adhesives remain amorphous in the secondary pigment (Fig.4 (B)). The XRD pattern of the secondary pigment shows the CoAl_2O_4 dominance indicating that there is no chemical reaction occurred between glass and pigment.

3.2.2 Thermal expansion analysis of low-melting-point glasses

Fig.5 shows the thermal expansion results of low-melting-point glasses 1[#] ~ 4[#]. The thermal expansion coefficients of the four low-melting-point glass samples are showed in Table 4, which are all close to $9.0 \times 10^{-6}/^\circ\text{C}$ (50~300 $^\circ\text{C}$), the thermal expansion coefficient of the plate glass substrate, with an acceptable difference of less than $0.3 \times 10^{-6}/^\circ\text{C}$. The consistency of thermal expansion coefficients can avoid the crack of glaze film during the process of cooling down after annealed.

Moreover, the glass transition temperatures (T_g) and the softening temperatures (T_s) of the four different glass samples are between 450 $^\circ\text{C}$ and 500 $^\circ\text{C}$, respectively. If the annealing temperature rises continuously

up and over T_s , the glass powders will be melted and turn into molten glass, which fix pigments on the surface of glass substrates. That indicates the practicability of setting the annealing temperature of coated samples at around 580 °C for 10 minutes. [32]

T_s and T_g slightly change with the different glass adhesives, which can attribute to the addition of TiO_2 and ZrO_2 in glass raw materials. Although the TiO_2 is an intermediates oxide, it can capture free oxides and transform coordination number from 6 to 4 in order to form tetrahedral structure unit $[TiO_4]$ which can participate in and strength the main Si-O network structures of glass. Meanwhile, the network former ZrO_2 owns high charge cationic Zr^{4+} and clusters negative oxygen ions O^{2-} , which can decrease the quantity of free oxides as well as the ratio of O/Si of $[SiO_4]$ and also enhance the stability of network structures. So the addition of small amount of TiO_2 and ZrO_2 will lead to the decrease of T_s and T_g , without affecting the thermal expansion coefficients substantially.

3.2.3 Particle size analysis of secondary pigment

Particle size, distribution of secondary particles, glass adhesive addition and milling time were studied and the results are displayed in Fig.6. Fig.6 (a) and (c) show that adding more glass adhesives or prolonging milling time can reduce the amount of big particles or agglomerates and lead to a narrow, log-normal size distribution. After milling for 16 h, the peak position of distribution graphs decreases

gradually to 459 nm from Fig.6 (c), meanwhile, similar results are obtained when the glass adhesive content increases to 91%. Additionally, the changing trends of mean particle sizes are showed in Fig.6 (b) and (d). It's evident that a same decline trend can be observed in both graphs (b) and (d), that's to say, the ideal mean particle size (around 500 nm) of secondary pigments can be prepared by means of increasing glass adhesive additions and milling time, separately or jointly.

The surface morphology and particle size distribution of the secondary pigments are important factors to the optical dispersion in a medium. [9] SEM micrographs of the secondary pigments with 91% of glass content and milled for 16h are shown in Fig. 7 (a) and (b), respectively. Fig.7 (a) shows that the particles in the secondary pigment with a 91% of glass content have an irregular shape with a wide size distribution ranging from 100 nm to 1 μ m with the mean particle size about 0.78 μ m. In addition, Fig.7 (b) illustrates the particle size distribution of secondary pigment after being milled for 16 h, and the same irregular shape can be observed, but the mean particle size is about 0.50 μ m. Therefore, it can be concluded that the way of increasing the milling time is efficient.

3.3 Glass ink

3.1 Viscosity of the prepared glass ink

Viscosity mainly affects the rheological characteristics of the glass ink when it circulates through the capillary nozzles of printer. A high viscosity could lead to an insufficient jet of ink, whereas a significantly small viscosity could degrade inner resistance of the ink, which makes the ink drop crescent shaped, resulting in damped oscillation. [2, 33] The viscosity of prepared blue glass ink was measured to be 28.45 mPa·s at room temperature, which allowed the glass ink to be printed well when flowing through the nozzles of the printer head and forming drops with proper physics and fluid mechanics performance during the printing process. [34, 35]

3.2 Surface tension of the prepared glass ink

Surface tension is another physical parameter measured for the printing performance of the prepared inks, which mainly affects the decomposition into fine drops of glass ink efflux through the capillary tube of the printer nozzle during printing process. The diethylene glycol monobutyl ether, as a major phase in the glass ink formulation, plays a decisive role in controlling the surface tension. According to recent literatures, the suitable range for surface tension is in between 20 to 70 mN·m⁻¹. [3, 11] The surface tension of the prepared blue glass ink was measured to be 29.18 mN·m⁻¹ at pH = 7.5, placing it within a range of the preferred value for ink-jet printing.

3.3 Main required properties for drop-on-demand printing ink

Particle size, viscosity, surface tension and pH are the four basic properties to evaluate whether the ink is suitable for drop-on-demand ink-jet printing. Limiting the particle size less than $1\mu\text{m}$ would effectively avoid blockages in nozzles of the printer. Viscosity mainly affects the flowing property of ink both in cartridge and pipe, while surface tension mainly controls the drop-forming process from the nozzle. The alkaline ink can prevent the printing nozzles being corroded. Table 5 shows the comparison of main required physical and chemical properties of drop-on-demand ink and blue glass ink. The results show that these physical and chemical values of our blue glass ink are within the normal ranges of the drop-on-demand printing ink, [11] indicating that our blue glass ink is applicable in ink-jet printing.

3.4 SEM analysis of cross section of the coating sample

SEM cross section images of the coating samples are shown in Fig.8, which clearly demonstrate the close connection between the ink layer and the substrate without any cracks or air pores. Fig.8 (a) shows the cross-sectional uniformity in the thickness of the ink layer on the plate glass slides, and at the same time, shows that the nano- CoAl_2O_4 pigments are well dispersed in the glaze layer. The interface between the glass and the glaze is displayed in Fig.8 (a) and (b). Two SEM images show a good

1 bonding between ink materials and the glass substrate, thanks to the
2
3 assistance of low melting point glass phase.
4
5
6

7 **4 Conclusions**

8
9

10 We have demonstrated in this paper that a stable nano- CoAl_2O_4 ink
11
12 that meets the ink-jet printing requirements is successfully synthesized by
13
14 mechanically grinding pigments and glass phase powders.
15
16
17

18 (a) The optimal reaction temperature for synthesizing CoAl_2O_4
19
20 pigment by solid-state reaction was 1300 °C and the $L^*a^*b^*$ values of
21
22 CoAl_2O_4 pigment were 35.75, -0.75, -24.51, respectively, indicating a
23
24 blue color.
25
26
27

28 (b) Glass adhesive of $\text{ZnO-B}_2\text{O}_3\text{-SiO}_2$ system was used to enhance
29
30 the binding of pigments on the surface of the substrates. T_g and T_s of
31
32 glass adhesive are at about 450 °C and 500 °C, respectively. The thermal
33
34 expansion analysis is about $9.0 \times 10^{-6}/^\circ\text{C}$ (50~300 °C), similar to that of
35
36 glass substrate, ensuring the crack-free coating
37
38
39
40
41
42

43 (c) Small particles that are in favor of ink-jet printing can be
44
45 obtained by milling pigment and glass adhesives together for 16 h.
46
47
48

49 (d) Surface tension of the prepared blue glass ink was measured to
50
51 be $29.18 \text{ mN}\cdot\text{m}^{-1}$ at pH=7.5, while viscosity of this glass ink was
52
53 $8.21 \text{ mPa}\cdot\text{s}$, which fall in the range of the preferred values for ink-jet
54
55 printing glass inks.
56
57
58
59
60
61
62
63
64
65

(e) Coated samples show that pigments are well dispersed in the ink layer and the prepared glass ink binds well on the surface of plate glass materials, enhancing the mechanical strength of the ink layer.

Acknowledgements

The authors acknowledge the financial support given by Glass and Technology Research Institute of Shahe.

References

- [1] Hosseini ZM, Soleimani-Gorgani A (2012) Ink-jet printing of micro-emulsion TiO₂ nano-particles ink on the surface of glass. J Eur Ceram Soc 32: 4271-4277
- [2] Soleimani-Gorgani A, Ghahari M, Peymannia M (2015) In situ production of nano-CoAl₂O₄ on a ceramic surface by ink-jet printing. J Eur Ceram Soc 35: 779-786
- [3] Zhao X, Evans JRG, Edirisinghe MJ, Song JH (2003) Formulation of a ceramic ink for a wide-array drop-on-demand ink-jet printer. Ceram Int 29: 887-892
- [4] Grau J, Cima M, Sachs E (1996) Fabrication alumina molds for slip casting and 3-D printing. Ceram Ind 146(7): 22-27
- [5] Teng WD and Edirsinghe MJ (1998) Development of ceramic inks for direct continuous jet printing of ceramics. Ceram Trans 81(4): 1033-1036
- [6] Kosmala A, Wright R, Zhang Q, Kirby P (2011) Synthesis of silver nano particles and fabrication of aqueous Ag inks for inkjet printing. Mater Chem Phys 129: 1075-1080
- [7] Menning M, Kalleder A, Jonschker G, Schmidt H (1997) Sol-gel coatings for the substitution of fluoride or lead containing white decorations on glass. J Non-Cryst Solids 218: 395-398
- [8] Kettle J, Lamminmäki T, Gane P (2010) A review of modified surfaces for high speed inkjet coating. Surf Coat Technol 204: 2013-2109
- [9] Chouiki M, Schoeftner R (2011) Inkjet printing of inorganic sol-gel ink and control of the geometrical and characteristics. J Sol-Gel Sci Technol 58: 91-95

- [10] Cavalcante PMT, Dondi M, Guaini G, Raimondo M, Baldi G (2009) Colour performance of ceramic nano-pigments *Dyes & Pigment* 80: 226-232
- [11] Gardini D, Dondi M, Costa AL, Matteucci F, Blosi M, Galassi C (2008) Nano-sized ceramics inks for drop-on-demand ink-jet printing in quadrichromy. *J Nanosci Nanotechnol* 8 (4) : 1979-1988
- [12] Fasaki I, Siamos K, Arin M, Lommens P, Van Driessche I, Hopkins SC, Glowacki BA, Arabatzis I (2012) Ultrasound assisted preparation of stable water-based nanocrystalline TiO₂ suspensions for photocatalytic applications of inkjet-printed films. *Appl Catal A* 411-412: 60-69
- [13] Akdemir S, Ozel E, Suvaci E (2011) Solubility of blue CoAl₂O₄ ceramic pigments in water and diethylene glycol media. *Ceram Int* 37: 863-870
- [14] Ma SH, Matrick H, Shor AC, Spinelli HJ, Sheard ME, Hochberg J (1993) Aqueous pigmented ink for ink jet printer. US Patent 5221334
- [15] Guo YJ, Zhou ZJ, Yang ZF (2002) Physicochemical properties of coloured ceramic ink used for continuous ink-jet printing by sol-gel method. *China Ceramic* 38: 17-19
- [16] Jovaní M, Domingo M, Machado TR, Longo E, Mir HB, Cordoncillo E (2015) Pigments based on Cr and Sb doped TiO₂ prepared by microemulsion-mediated solvothermal synthesis for inkjet printing on ceramic. *Dyes & Pigment*. 116: 106-113
- [17] Merikhi J, Jungk HO, Feldmann C (2000) Sub-micrometer CoAl₂O₄ pigment particles-synthesis and preparation of coatings. *J Mater Chem* 10: 1311-1314

- [18] Dondi M, Blosi M, Gardini D, Zanelli C (2012) Ceramic pigments for digital decoration inks: an overview. *Ceramic Forum International* 8: 59-64
- [19] Kim JH, Son BR, Yoon DH, Hwang KT, Noh HG, Cho WS, Kim US (2012) Characterization of blue CoAl_2O_4 nano-pigment synthesized by ultrasonic hydrothermal method. *Ceram Int* 38: 5707-5712
- [20] Kuscer D, Ozkol G, Trefalt G, Kosec M (2012) Formulation of an aqueous titania suspension and its patterning with ink-jet printing technology. *J Am Ceram Soc* 95: 487-493
- [21] Burdett JK, Price GD, Price SL (1982) Role of the crystal-field theory in determining the structures of spinels. *J Am Chem Soc* 104: 92-94
- [22] Wang C, Liu S, Liu L, Bai X (2006) Synthesis of cobalt-aluminate spinels via glycine chelated precursors. *Mater Chem Phys* 96: 361-410
- [23] Manfredo LJ, McNally RN (1984) The corrosion resistance of high ZrO_2 fusion-cast Al_2O_3 - ZrO_2 - SiO_2 glass refractories in soda lime glass. *J Mater Sci* 19: 1272-1276
- [24] Matsuda A, Matsuno Y, Katayama S (1989) Weathering resistance of glass plates coated with sol-gel derived 9TiO_2 - 91SiO_2 films. *J Mater Sci* 8: 902-904
- [25] Cheng JS, Kang JF, Lou XC, Zhang XM, Liu K (2015) Effect of TiO_2 on crystallization of the glass ceramics prepared from granite tailings. *Journal of Wuhan University of Technology-Mater Sci Ed* 30: 22-26
- [26] Cheng HZ, Lin HJ, Wang MC, Lu P (2015) Influences of TiO_2 addition on the crystallization behavior, microstructure and magnetic properties of

1 $\text{Li}_2\text{O}-\text{MnO}_2-\text{Fe}_2\text{O}_3-\text{CaO}-\text{P}_2\text{O}_5-\text{SiO}_2$ glasses. Metal Mater Trans A 46: 2040-2050
2

3 [27] Strukelj E, Comte M, Roskosz M, Richet P (2015) Effect of zirconium on the
4 structure and congruent crystallization of a super cooled calcium aluminosilicate
5 melt. J Am Chem Soc 98: 1942-1950
6
7
8
9

10 [28] Greenstein LM (1988) Properties and Economics, in Pigment Handbook, ed. by
11 P.A. Lewis. Volume 1, 2nd pp829-858
12
13
14
15
16

17 [29] Granados NB, Yi E, Laine R, Baena ORJ (2015) CoAl_2O_4 blue nanopigments
18 prepared by liquid-feed flame spray pyrolysis method. Matéria, pp580-587
19
20
21
22

23 [30] Ahmed IS, Dessouki HA, Ali AA (2008) Synthesis and characterization of new
24 nano-particles as blue ceramic pigment, Spectrochim Acta Part A 71: 616-620
25
26
27

28 [31] Cunha JD, Melo DMA, Martinelli AE, Melo MAF, Maia I, Cunha SD (2005)
29 Ceramic pigment obtained by polymeric precursors. Dyes & Pigments. 65: 11-14
30
31
32

33 [32] Tool AQ (1946) Relation Between Inelastic Deformability and Thermal
34 Expansion of Glass. J Am Chem Soc 29: 240-253
35
36
37
38

39 [33] Peymannia M, Soleimani-Gorgani A, Ghahari M, Najafi F (2014) Production of a
40 stable and homogeneous colloid dispersion of nano- CoAl_2O_4 pigment for
41 ceramic ink-jet ink. J Eur Ceram Soc 34: 3119-3126
42
43
44
45
46

47 [34] Derby B (2010) Inkjet printing of functional and structural materials-fluid
48 property requirements, feature stability and resolution. Annu Rev Mater Sci 40:
49 395-414
50
51
52
53
54

55 [35] Martin GD, Hoath SD, Hutchings IM (2008) Inkjet printing-the physics of
56 manipulating liquid jets and drops. J Phys Conf Ser 105: 012001
57
58
59
60
61
62
63
64
65

Figure captions

Fig.1 The flowchart of the whole preparing processes of blue glass ink and glass surface coating

Fig.2 XRD patterns of the CoAl_2O_4 powders at different reaction temperatures: (a) 900 °C; (b) 1100 °C; (c) 1200 °C; (d) 1300 °C

Fig.3 Pictures of the prepared primary pigments (a) ~ (d) and coated sample (e)

Fig.4 XRD patterns of (A) low-melting-point glass (1) ~ (4);

(B) Primary pigment (d) and secondary pigment (88%)

Fig.5 Thermal expansion curves of low-melting-point glasses 1# ~ 4#;

Fig.6 Size distribution curves of secondary pigments under different conditions:

(a) Effect of different glass adhesives additions on distribution of secondary pigments;

(b) Changing trend of mean particle size with different glass adhesive additions;

(c) Effect of different milling times on distribution of secondary pigments;

(d) Changing trend of mean particle size with different milling times;

Fig.7 SEM micrographs of the milled pigments with different treatments: (a) 91% glass contents; (b) 16h of milling

Fig.8 SEM images of printing sample: magnification X2000(a) and X5000(b)

Figures:

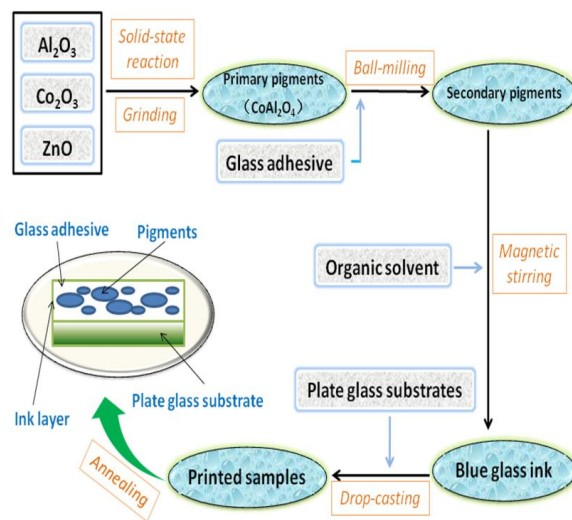


Fig. 1

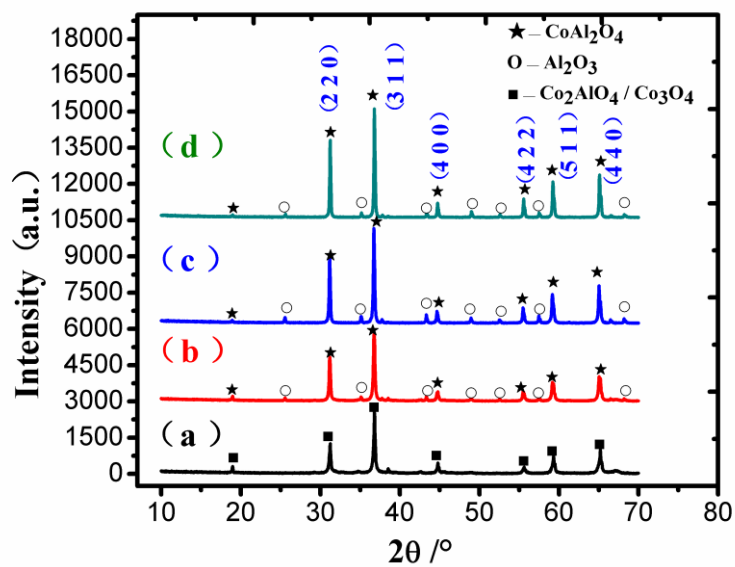


Fig. 2

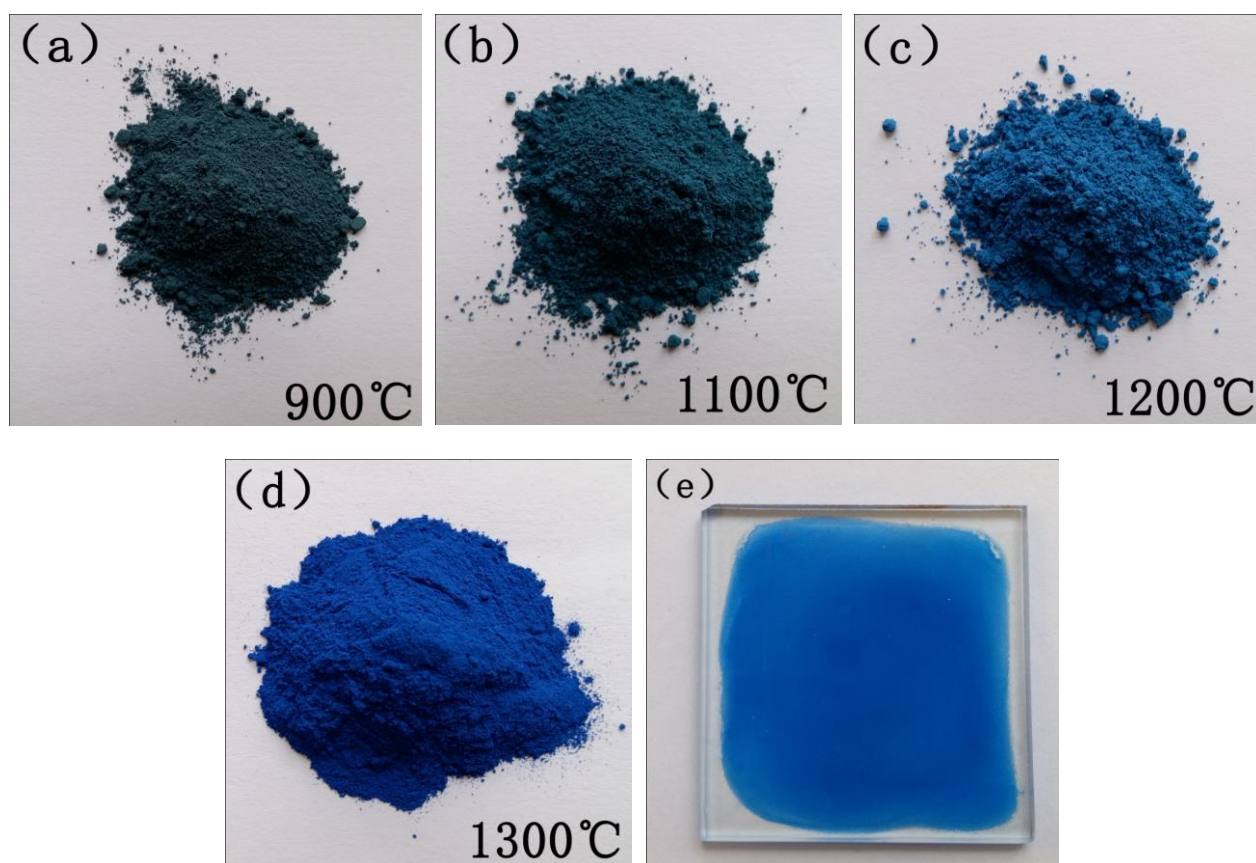


Fig. 3 (a), (b), (c), (d) and (e)

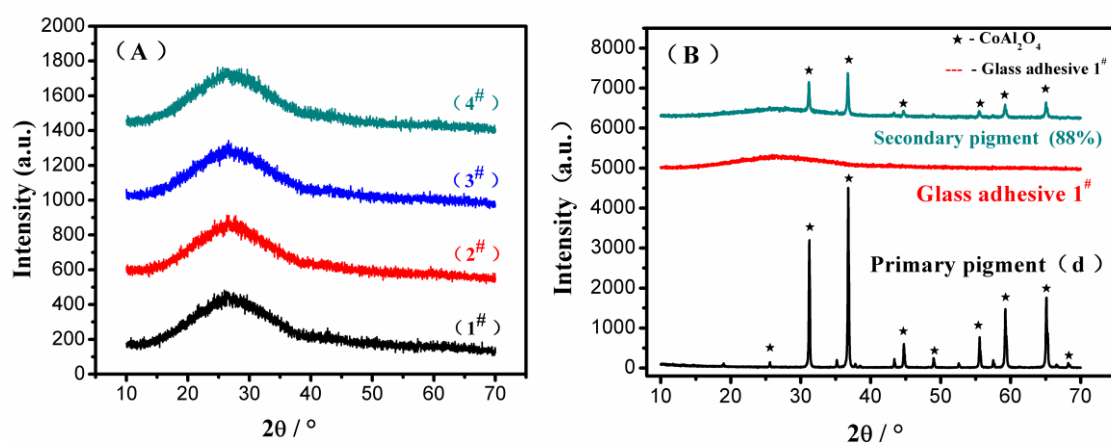


Fig. 4 (A) and (B)

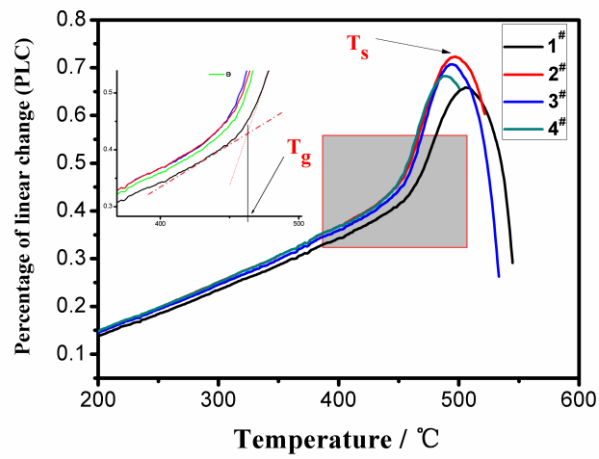


Fig. 5

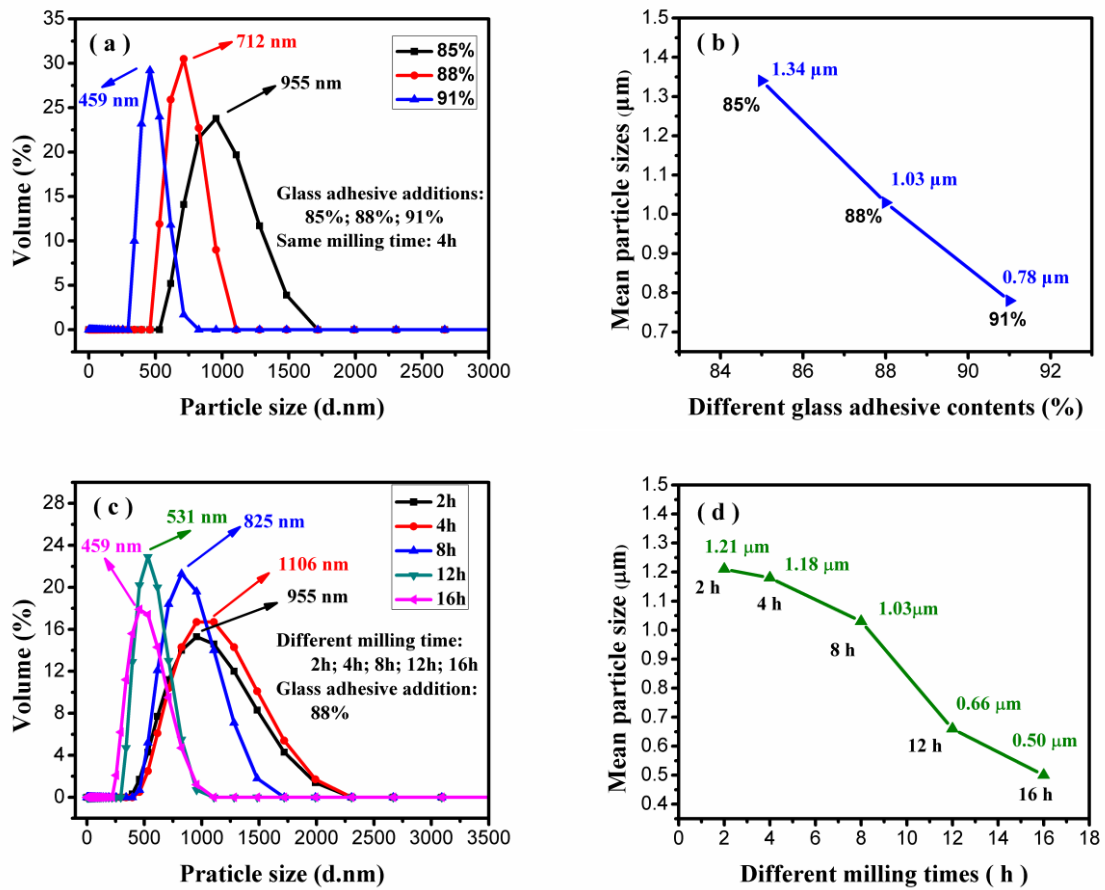


Fig. 6 (a), (b), (c) and (d)

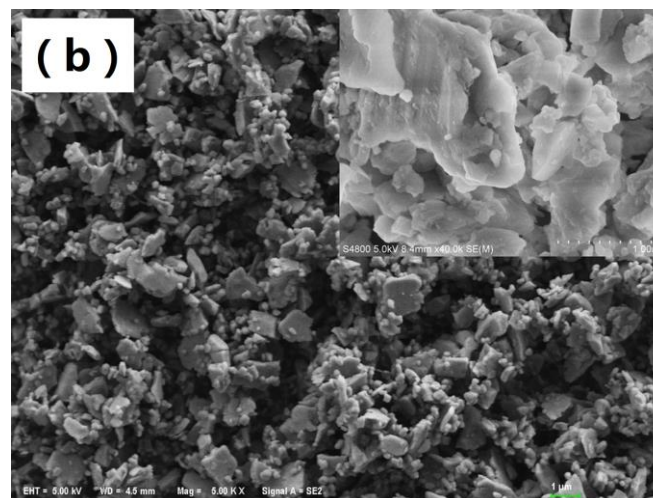
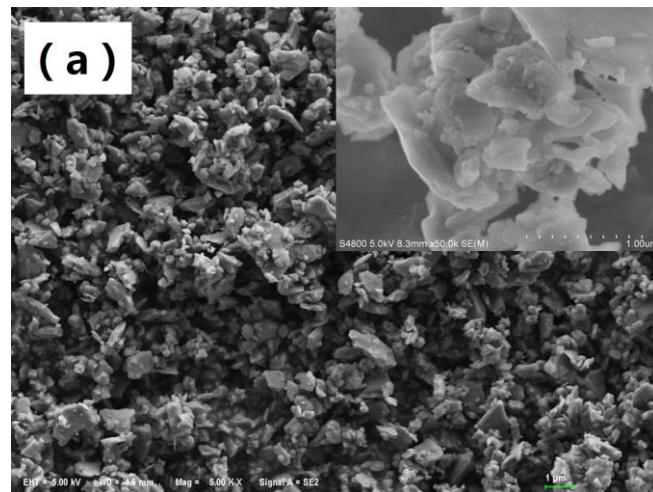


Fig. 7 (a) and (b)

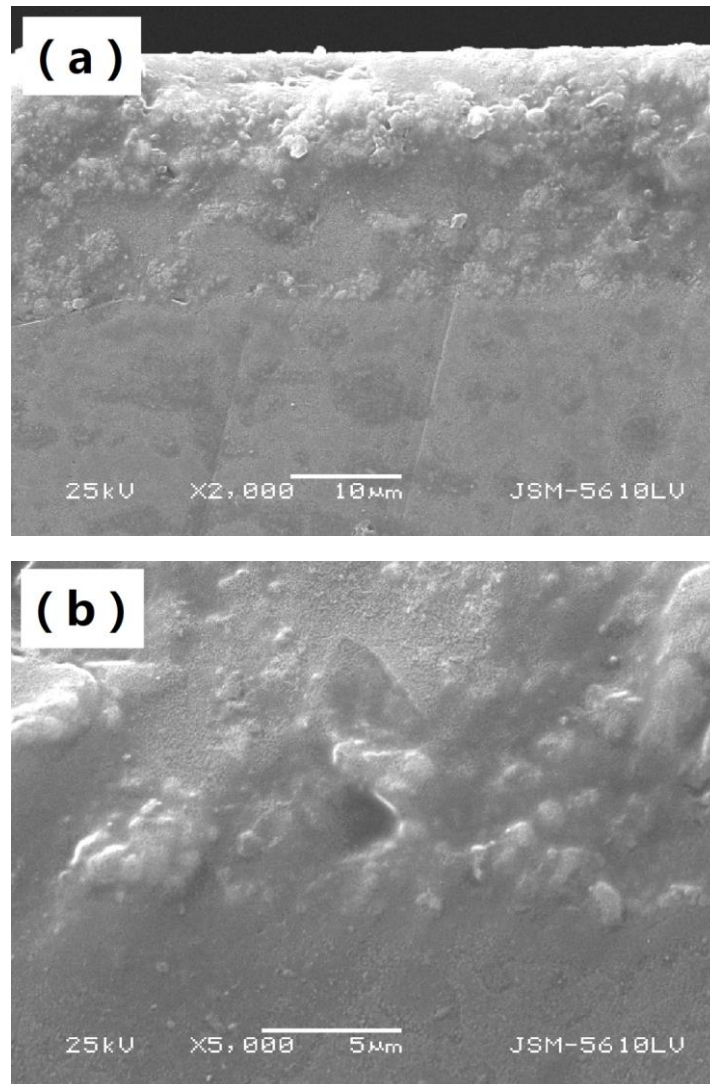


Fig. 8 (a) and (b)

Table captions:

Table 1 Chemical compositions of low-melting-point glass /wt%

Table 2 Chemical compositions of the prepared blue glass ink/wt%

Table3 L*a*b* values of primary pigments (a), (b), (c) and (d)

Table 4 Thermal expansion coefficients of the four different glass adhesives

Table5 Comparison of main required properties of inks

Tables:

Table 1

	SiO ₂	B ₂ O ₃	ZnO	Al ₂ O ₃	Li ₂ O	Na ₂ O	K ₂ O	CaO	BaO	TiO ₂	ZrO ₂
GA-1	41.24	17.53	17.53	3.08	6.19	6.70	3.61	2.57	1.55	2	1
GA-2	41.24	17.53	17.53	3.08	6.19	6.70	3.61	2.57	1.55		1
GA-3	41.24	17.53	17.53	3.08	6.19	6.70	3.61	2.57	1.55	2	
GA-4	41.24	17.53	17.53	3.08	6.19	6.70	3.61	2.57	1.55		

Table 2

Solvent	Primary pigment		4.29%
	Glass adhesive		31.43%
	1,2-Propylene glycol diacetate		17.36%
	Diethylene glycol monobutyl ether		41.76%
	Polyacrylate		3.54%
	Zinc isoocatanoate		1.61%
	Polysiloxane		0.01%

Table3

Primary pigment	L*	a*	b*
(a)	26.24	-0.42	-7.84
(b)	28.72	-0.48	-16.11
(c)	33.26	-0.75	-20.34
(d)	35.75	-1.59	-24.51

Table 4

Thermal expansion coefficient	
1#	8.704*10 ⁻⁶
2#	9.246*10 ⁻⁶
3#	9.086*10 ⁻⁶
4#	9.229*10 ⁻⁶

Table5

	Drop-on-demand printing ink	Blue glass ink
Maximum particle size	< 1μm	500 nm
Viscosity (mPa·s)	1 ~ 30	8.21
Surface tension (mN·m ⁻¹)	20 ~ 70	29.18
pH	7 ~ 12	7.5

Preparation and Characterization of a Stable Nano-Sized $\text{Zn}_x\text{Co}_{1-x}\text{Al}_2\text{O}_4$ Ink for Glass Decoration by Ink-jet Printing

Peng, Xiaojin

2017-06

Attribution-NonCommercial 4.0 International

Xiaojin Peng, Qi Zhang, Jinshu Cheng, Jian Yuan Ya Wu and Junnan Jie. Preparation and Characterization of a Stable Nano-Sized $\text{Zn}_x\text{Co}_{1-x}\text{Al}_2\text{O}_4$ Ink for Glass Decoration by Ink-jet Printing. *Fizika i Khimiya Stekla / Glass Physics and Chemistry*, May 2017, Vol.43, Iss.3, pp246-256
<http://dx.doi.org/10.1134/S1087659617030105>

Downloaded from CERES Research Repository, Cranfield University